Weakly solvated PEG-functionalized silica nanoparticles with liquid-like behavior

A. B. BOURLINOS*
Institute of Materials Science, NCSR Demokritos, Ag. Paraskevi Attikis, Athens 15310, Greece
E-mail: bourlinos@ims.demokritos.gr

S. RAY CHOWDHURY, D. D. JIANG
Department of Materials Science and Engineering, Cornell University, Ithaca 14853, NY, USA

Q. ZHANG
School of Chemical and Biomolecular Engineering, Cornell University, Ithaca 14853, NY, USA

Surface engineering of nanoparticles has fueled the evolution of nanoscience and nanotechnology through the design of new materials that, depending on their surface modifier, exhibit a range of functional properties and applications [1–6]. However, in all instances in the absence of solvents the functionalized nanoparticles behave solid-like. Therefore, excess of solvent is required in order to obtain colloidal fluids and fluidity where typically the concentration of the functionalized nanoparticles does not exceed 50% w/w (e.g. Ludox colloidal dispersions). In the present communication we describe the synthesis of weakly solvated PEG-functionalized silica nanoparticles [PEG: poly(ethylene glycol)] with liquid-like behavior, thus representing a unique case of a colloidal fluid with unusually low solvent content (5% w/w), and in turn, high functionalized nanoparticle concentration (95% w/w). To the best of our knowledge, functionalized nanoparticles exhibit no fluidity or dispersibility even if containing a small amount of solvent (<10%). Instead, they behave like a powder, wax or paste.

The modification of the silica nanoparticles takes place by covalent grafting of the neutral, hydrophilic silane $(CH_3O)_3Si(CH_2)_3O(CH_2CH_2O)_{6\text{–}9}CH_3$ onto silica surface through the formation of Si–O–Si bridges. In the literature the surface functionalization of a variety of nanoparticles with PEG-based ligands has been described [7–12], however, no fluidity/dispersibility in the presence of a small amount of solvent has been observed for any of these cases. Typically, in 3.5×10^{-6} m^3 of colloidal silica (Ludox SM, 34 wt.% SiO_2, 7 nm, pH = 10) diluted with 2×10^{-5} m^3 H_2O, 2.5 g of $(CH_3O)_3Si(CH_2)_3O(CH_2CH_2O)_{6\text{–}9}CH_3$ (90%, Gelest) were added. The sol was placed in a sealed plastic bottle and heated at 70 °C for 24 hr. After completion of the reaction, the clear sol was extracted thoroughly with toluene. After extraction, the aqueous layer was isolated and dried at 70 °C to one-fifth of its volume (solidification of the concentrate was avoided). The remaining liquid was further extracted several times with toluene. The as-obtained liquid was dispersed in 10^{-5} m^3 of acetone and centrifuged in order to remove any insoluble particles. The supernatant dispersion was collected and dried at room temperature for 2 days followed by 2 days vacuum drying to finally produce an optically transparent, viscous liquid (Silpeg7). Silpeg7 is dispersible in water, acetone and tetrahydrofuran (THF).

Solidification occurs after prolong vacuum drying at room temperature or heating at 90 °C at ambient conditions. It is possible that solvent evaporation and simultaneous condensation reactions between free silanol groups from the surface modifier, e.g. from partially grafted oligomers, among adjacent particles contribute to solidification. The condensation reactions were unveiled by infrared (IR) spectroscopy from a relative decrement of the characteristic for the Si-OH group band at 950 cm^{-1}. In addition, the solid does not redisperse in solvents thus signaling for cross-linking reactions. This irreversible liquid-to-solid transition may find applications in thermosetting films, adhesives and molded objects. Colored versions of the latter are also possible since the liquid can easily dissolve dye molecules (e.g. methylene blue).

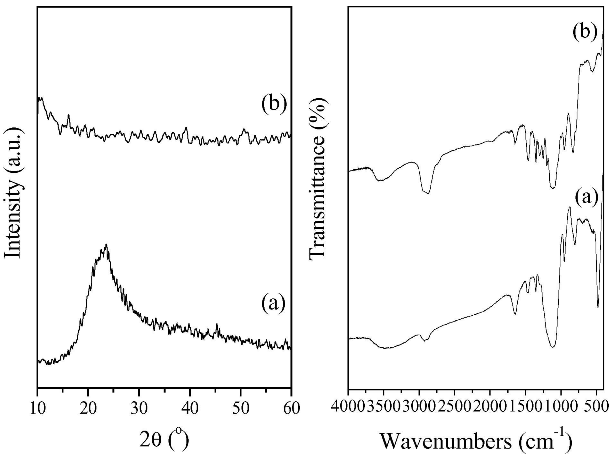

Figure 1 Left: XRD patterns of Silpeg7 (a) and of the sample holder (b) (CuKα, $\lambda = 0.154$ nm). Right: IR spectra of Silpeg7 (a) and neat PEG-tailed silane (b).

---

* Author to whom all correspondence should be addressed.

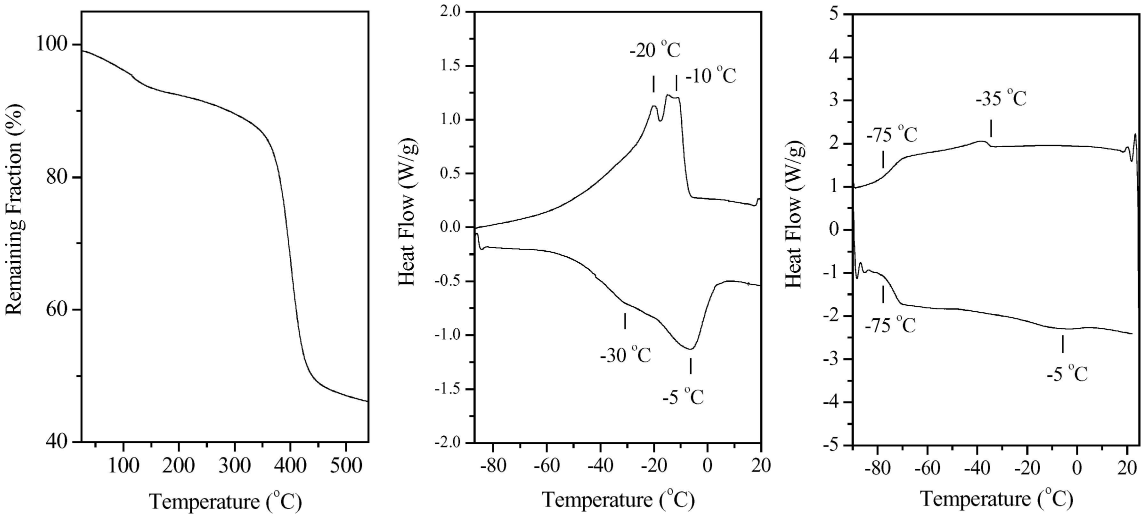

Figure 2 TGA trace of Silpeg7 (left) and DSC plots of the neat PEG-tailed silane (middle) and Silpeg7 (right) (heating rate: 10 °C min^{-1}).

The X-ray diffraction (XRD) pattern of Silpeg7 shown in Fig. 1, left, reveals the presence of amorphous silica nanoparticles, as evidenced by a broad reflection centered at 2θ–22° (note that the XRD pattern of the sample holder itself does not show the particular peak). The material is amorphous in the low 2θ region, i.e. 1–10 °, as a result of its liquid-state nature. The silane grafting is confirmed by the presence of the characteristic absorption bands due to CH_3, CH_2, and C–O vibrations. In addition, the sample shows sharp absorption bands at 1100 and 500 cm^{-1} corresponding to the silica network (Fig. 1, right). Therefore the XRD and IR data confirm the presence of PEG-functionalized silica nanoparticles in Silpeg7.

The thermal gravimetric analysis (TGA) trace of Silpeg7 shows a weight loss above 200 °C attributed to the decomposition of the PEG modifier (total 45% w/w) (Fig. 2, left). By a rough estimation, we find a surface coverage of 2–3 silane molecules per nm^2 silica surface, which is 1.5 times higher than the theoretically expected. The liquid contains a small amount of water (~5% w/w) that provides solvent plasticizing. Most likely, the water molecules interact with the oxygen atoms of the PEG chains through hydrogen bonding thus solvating them. Differential scanning calorimeter (DSC) analysis shows a prominent, reversible second order transition at -75 °C, most likely corresponding to the glass transition (T_g). The low T_g in conjunction with the presence of a small amount of solvent explains the liquid-state appearance of Silpeg7 (Fig. 2, right). On the contrary, the un-grafted silane itself exhibits two first order transitions at -20 and -5 °C in the heating direction and another two at -10 and -20 °C in the cooling direction, corresponding to the melting/(solidification temperature of the silane, respectively (Fig. 2, middle.) (The observed temperature distribution arises from the variation of the ethylene glycol units per silane molecule, i.e. 6–9 ethylene glycol units per molecule). Therefore the DSC analysis clearly differentiates between the silane and Silpeg7.

Transmission electron microscopy (TEM) imaging of Silpeg7 reveals the presence of uniform sized spherical nanoparticles of 7 nm in diameter, suggesting preservation of the nanostructure in the liquid state (Fig. 3). The TEM image was taken by dispersing the liquid in acetone (5% w/v), placing few drops of the dispersion on a copper greed and evaporating acetone. Notably, a ~2.2 nm thickness mantle is observed around the particles, which is attributed to the PEG-tailed modifier. Assuming a size of ~0.3 nm per ethylene glycol unit [13] (–CH_2–CH_2–O–) and 6–9 ethylene glycol units per silane we conclude that the full length of the attached PEG chains should be in the range of 2–3 nm. The optical transparency of the liquid is probably due to a refractive index match and the corresponding size of the nanoparticles, which eliminate scattering.

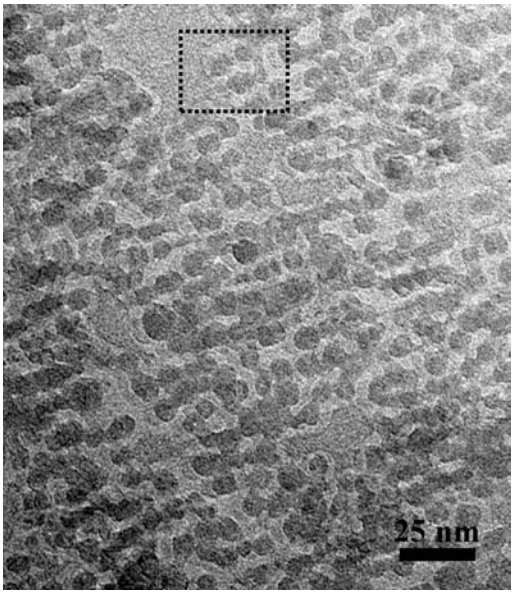

Figure 3 TEM image of Silpeg7 (the dot square indicates the modifier's sheath around the nanoparticles).

Concerning the rheological behavior of Silpeg7 at room temperature, the shear-loss modulus G'' (1200 Pa) is higher than the storage modulus G' (640 Pa) suggesting a viscous-like, fluid behavior (strain amplitude: $\gamma = 1\%$, angular frequency: $\omega = 1$ s^{-1}). Furthermore, the viscosity versus angular frequency at room temperature ($\gamma = 2\%$) normally decreases with increasing frequency with values commensurate of the

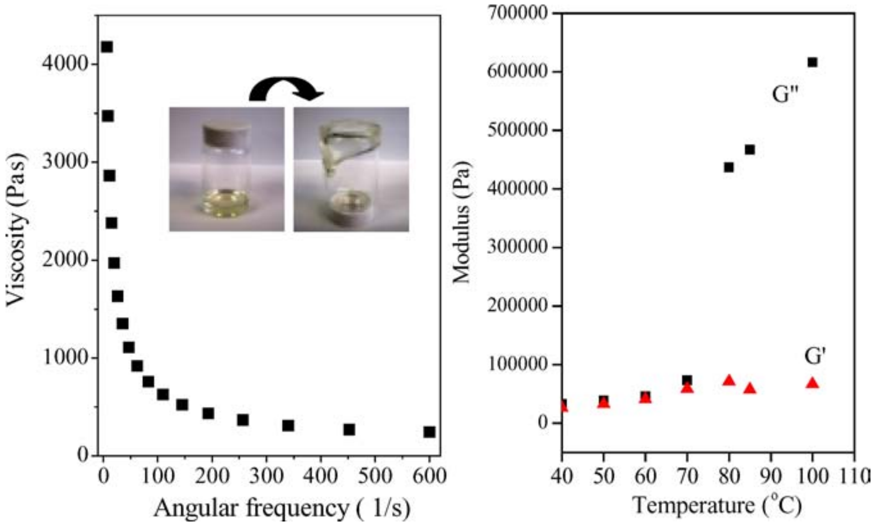

Figure 4 Viscosity versus angular frequency at room temperature for Silpeg7 (left). Temperature-depended storage and loss moduli plots (right).

viscous-like behavior of Silpeg7 (Fig. 4, left, and inset). Fig. 4, right, presents the temperature dependence of loss and storage moduli. We observe that at higher temperatures the storage modulus becomes prominent, thus signaling solidification of the sample.

The high organic content of the material and plasticizing provided by the PEG-tailed modifier and solvent must play a key role in isolating the as-functionalized nanoparticles in liquid form, where the hydrated modifier provides enough "solvent" for the dispersion of the functionalized nanoparticles. In another view, the molten organic shell acts like a lubricant between the nanoparticles. A lower organic loading, i.e. 27% w/w (surface coverage: 1–2 silanes per nm^2), and same water content result in a non-meltable powder that is dispersible in water but not in acetone. Moreover, silica nanoparticles 22 nm in size (Ludox TM-50) treated similarly as for the Silpeg7 case result in a gel-like product (40% w/w organic, 10% w/w H_2O) that does not flow or melt. On the other hand, silica nanoparticles 12 nm in size (Ludox HS-30) afford a liquid (43% w/w organic, 7% w/w H_2O) quite comparable in behavior with Silpeg7. These results reflect also the effect of particle size on the physical appearance of the as-functionalized nanoparticles. It is expected that the smaller the particle size the higher the fluidity of a sample under comparable organic and solvent contents.

In summary, weakly solvated PEG-functionalized silica nanoparticles with liquid-like behavior were obtained by functionalizing the nanoparticles with a neutral, hydrophilic PEG-tailed silane. This finding introduces a new class of low solvent content colloidal fluids and seems extendable to different types of nanoparticles provided that they are below a certain size, possess relatively low density and are amenable to surface modification.

Acknowledgements

We gratefully acknowledge the support by the Cornell Center for Materials Research (CCMR)

References

1. C. M. NIEMEYER, *Angew. Chem. Int. Ed.* **40** (2001) 4128.
2. M. P. PILENI, *J. Phys. Chem. B* **105** (2001) 3358.
3. A. L. ROGACH, D. V. TALAPIN, E. V. SHEVCHENKO, A. KORNOWSKI, M. HAASE and H. WELLER, *Adv. Funct. Mater.* **12** (2002) 653.
4. V. TOHVER, A. CHAN, O. SAKURADA and J. A. LEWIS, *Langmuir* **17** (2001) 8414.
5. E. C. SCHER, L. MANNA and A. P. ALIVISATOS, *Phil. Trans. R. Soc. Lond. A* **361** (2003) 241.
6. D. S. GINGER, H. ZHANG and C. A. MIRKIN, *Angew. Chem. Int. Ed.* **43** (2004) 30.
7. G. BILLANCIA, D. WOUTERS, A. A. PRECUP and U. S. SCHUBERT, *Polym. Mater. Sci. Eng.* **85** (2001) 508.
8. Q. ZHANG and L. A. ARCHER, *Langmuir* **18** (2002) 10435.
9. H. OTSUKA, Y. NAGASAKI and K. KATAOKA, *Adv. Drug Deliver. Rev.* **55** (2003) 403.
10. N. KOHLER, G. E. FRYXELL and M. ZHANG, *J. Am. Chem. Soc.* **126** (2004) 7206.
11. P. J. COSTANZO, T. E. PATTEN and T. A. P. SEERY, *Chem. Mater.* **16** (2004) 1775.
12. T. ISHII, H. OTSUKA, K. KATAOKA and Y. NAGASAKI, *Langmuir* **20** (2004) 561.
13. H. J. KREUZER and M. GRUNZE, *Europhys. Lett.* **55** (2001) 640.

Received 22 February
and accepted 1 April 2005